

RePPL: Recalibrating Perplexity by Uncertainty in Semantic Propagation and Language Generation for Explainable QA Hallucination Detection

Yiming Huang^{1*}, Junyan Zhang^{1*}, Zihao Wang², Biquan Bie³,
Xuming Hu^{1,2}, Yi R. (May) Fung², Xinlei He^{1,†}

¹The Hong Kong University of Science and Technology, Guangzhou,

²The Hong Kong University of Science and Technology, ³Independent Researcher

†Correspondence: xinleihe@hkust-gz.edu.cn

Abstract

Large Language Models (LLMs) have become powerful, but hallucinations remain a vital obstacle to their trustworthy use. While previous works improved the capability of hallucination detection by measuring uncertainty, they all lack the ability to explain the provenance behind why hallucinations occur, i.e., which part of the inputs tends to trigger hallucinations. Recent works on the prompt attack indicate that uncertainty exists in semantic propagation, where attention mechanisms gradually fuse local token information into high-level semantics across layers. Meanwhile, uncertainty also emerges in language generation, due to its probability-based selection of high-level semantics for sampled generations. Based on that, we propose **RePPL** to recalibrate uncertainty measurement by these two aspects, which dispatches explainable uncertainty scores to each token and aggregates in **Perplexity**-style Log-Average form as total score. Experiments show that our method achieves the best comprehensive detection performance across various QA datasets on advanced models (average AUC of 0.833), and our method is capable of producing token-level uncertainty scores as explanations for the hallucination. Leveraging these scores, we preliminarily find the chaotic pattern of hallucination and showcase its promising usage.

1 Introduction

Since the milestone work ChatGPT (OpenAI, 2023) has revolutionized the fields of Language Generation, powerful Large Language Models (LLMs) are constantly updating and continuously shaping the text-driven automation in everyday applications like chatbots, document summarizers, and AI search engines. Despite these successes, one of the fatal shortcomings of LLMs is hallucination, i.e., factually incorrect or contextually inconsistent

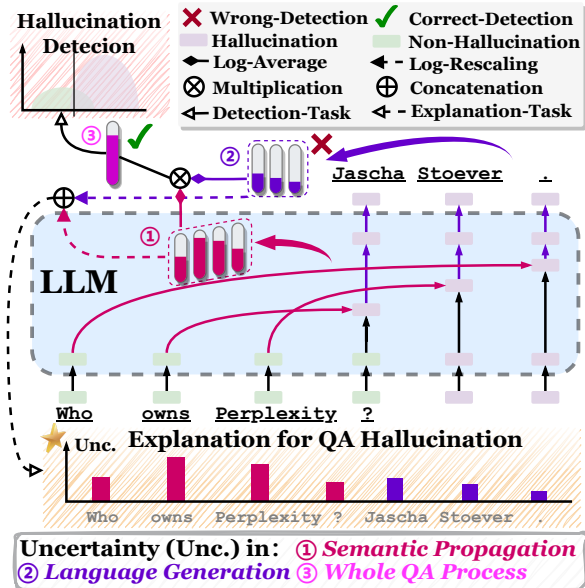


Figure 1: Illustration of our motivation. The LLM (Llama-3.1-8B-Instruct) generates a hallucinated answer “Jascha Stoever” to the question “Who owns Perplexity?”, with high-confidence (low-uncertainty) logits. This makes the detection hard for existing methods, while ours judges it correctly with the explanation.

outputs. Due to the urgent demand for trustworthiness in these LLM-based applications, detecting hallucination and figuring out how LLMs hallucinate is crucial to building robust AI systems. To tackle question answering (QA) hallucination in LLM, prior works (Ren et al., 2023; Liu et al., 2020; Lin et al., 2022; Malinin and Gales, 2021; Farquhar et al., 2024; Chen et al., 2024) identify the uncertainty of generations as the key point. These methods can be divided into two groups: logits-based and sampling-based methods. The logits-based methods (Ren et al., 2023; Liu et al., 2020; Lin et al., 2022) utilize the confidence of each token’s generation to accumulate uncertainty, while the sampling-based (Malinin and Gales, 2021; Farquhar et al., 2024; Chen et al., 2024) methods measure the discrepancy between sampled generations

* Equal contribution.

as uncertainty. However, these detection methods cannot explain why LLMs hallucinate and which part of the inputs triggers the hallucination. Our motivation stems from two observations. Firstly, recent works (Xu et al., 2024; Liu et al., 2024) about LLMs’ prompt attack applied to different parts of inputs can easily trigger various LLMs’ untrustworthy output, including hallucinations. Secondly, the confidences of generations represented by logits often vary between different tokens and different generations. This suggests that uncertainty arises both in semantic propagation, where attention gradually fuses local token information into high-level semantics across layers, and language generation, where the probability-based token generation selectively discards the remaining high-level semantics. As Figure 1 shows, we aim to combine these two aspects for both explainable and better hallucination detection. From this viewpoint, we propose **RePPL** to recalibrate uncertainty by these two perspectives with **Perplexity**-style aggregation. For the intrinsic semantic propagation, we utilize the attribution-based explainability method (Abnar and Zuidema, 2020; Chefer et al., 2021) to compute token-level uncertainty (inverse of confidence) by measuring token attribution discrepancies across sampled generations. For the extrinsic language generation, we normalize token confidence by the average generation length to make the confidence more distinct as Figure 1 depicts, uncertainty (or confidence) scores correspond to each token as an explanation. And we use **Perplexity**-style (Ren et al., 2023) aggregation that firstly rescales confidence into log form, then averages them all. We name these two total scores as **InnerPPL** and **OuterPPL**. Through multiplying them, we derive the recalibrated hallucination score **RePPL**. Experiments show that our method comprehensively outperforms baselines across QA datasets, achieving an average AUC of 0.833. It also faithfully explains hallucination through highlights of the uncertainty-inducing tokens. Meanwhile, we find the chaotic pattern of hallucination through statistical correlation between these uncertainty scores and attribution-based salience scores. To summarize, our contribution can be concluded in the following threefold:

1. We address the novel view to balance uncertainty in semantic propagation and language generation, which brings token-correspondence and hierarchical distinctness

to propose our innovative hallucination detection score **RePPL** with explainability.

2. Our proposed method **RePPL** achieved the leading performance in hallucination detection tasks. And it is robust under different hyperparameter settings and sampling options.
3. **RePPL**’s uncertainty scores are pioneering in explaining the hallucination triggered by both input prompts and output contents. It provides a faithful token-level explanation by indicating uncertainty-inducing tokens and serves as a useful statistical signal for analyzing attention disorder and hallucination patterns.

2 Related Works and Background

2.1 Uncertainty in Hallucination Detection

Uncertainty measurement (Fakour et al., 2024; Sun et al., 2017) is a classic research topic in the wide machine learning domain. It is highly related to out-of-distribution detection, which is inherently correlated to hallucination detection (Zhang et al., 2024; Ma et al., 2025). Uncertainty-based hallucination detection can be mainly sorted into two kinds. The first is the logits-based, like widely used **Perplexity** (Ren et al., 2023) and typical **Verbalize** (Lin et al., 2022) a.k.a. $P(\text{True})$, these methods exert confidence within logits to figure up uncertainty in a single generation. The second is the sampling-based, for instance, **Semantic Entropy** (Farquhar et al., 2024) and **EigenScore** (Chen et al., 2024). These methods take the discrepancy between different generations as uncertainty. Despite the effectiveness of these methods, they only pay attention to uncertainty in generation. It hinders them from exploiting the process of how input transforms into output, namely the semantic propagation, for better performance and potential explainability. In addition, we also notice the powerful probe-based method (Ji et al., 2024; Du et al., 2024; Wang et al., 2024). But they have two main shortcomings: 1. They need frequent adjustments with task-specific losses or hyperparameters for peak performance. 2. They lack transferability across updates of the model’s weight, resulting in unsuitability as an unsupervised hallucination indicator for scenarios like tracing hallucination risks of the LLM pretraining stage. We hence consider them more cost-effective for target LLMs and exclude them from comparison in Section 4.1.

2.2 Attribution Explanation

In the explainable AI (XAI) domain, attribution is an enduringly appealing topic as it indicates the salient part of the model’s inputs to the model’s prediction. For model-specific ones, Rollout (Abnar and Zuidema, 2020), GenAtt (Chefer et al., 2021), and AttnLRP (Achtibat et al., 2024) improve the attribution ability by utilizing attention maps among different layers of transformers. For model-agnostic ones, like LIME-style (Ribeiro et al., 2016) and Shapley-value-based (Lundberg and Lee, 2017; Lundberg et al., 2018), they need sufficient input perturbation for measuring the importance of absent tokens. Because model-specific methods need expensive gradients and model-agnostic methods need too many throughputs to guarantee their precision, they are intractable in explaining real-time hallucination detection. Therefore, we adopt simple maximum, average, and Rollout to pool attention maps as attribution across layers and heads. These attribution methods commonly generate an attribution map, and the row of this map represents the token-to-token contribution salience (scores). At the instance level, we attribute the uncertainty score expressing token-wise propensity to induce hallucinations rather than the salience score by the above methods, as the explanation of hallucination. At the macro-level, it is also useful to explore the underlying factors of the hallucination pattern, like prior works (Zhang et al., 2025; Ferrando et al., 2025; Yu et al., 2024; Orgad et al., 2024).

3 Methodologies

3.1 Attention-based Attribution

As Section 2.2 discussed, we choose the following three attention pooling strategies. The first is maximum pooling, abbreviated as **MaxPool**. Given attention maps of t tokens $\mathbf{A}^{(l)} \in \mathbb{R}^{h \times t \times t}$ across different attention heads \mathbf{h} of attention in layer \mathbf{l} in \mathbf{L} layers transformer-based LLM. We take the final attribution $\mathbf{R} \in \mathbb{R}^{t \times t}$ as:

$$\mathbf{R} = \text{MaxPool}(\mathcal{A}) = \text{Max}_l(\text{Max}_h(\mathcal{A})),$$

here, $\mathcal{A} = [\mathbf{A}_1, \mathbf{A}_2, \dots, \mathbf{A}_L]$ is the attention maps concatenation along the layer dimension and Max_d is the maximum selection among values along d dimension. Similarly, the average pooling **AvgPool** is (Avg_d is the average operation):

$$\mathbf{R} = \text{AvgPool}(\mathcal{A}) = \text{Avg}_l(\text{Avg}_h(\mathcal{A})).$$

As for Rollout (Abnar and Zuidema, 2020) pooling **RollPool**, it layer-wisely accumulates relevance from equal single-head attention $\bar{\mathbf{A}}$ as attribution, meanwhile, it also considers the relevance in the residual part. We adopt same enhancement in GenAtt (Chefer et al., 2021) as follows:

$$\begin{aligned} \mathbf{R}^{(l)} &\leftarrow \mathbf{R}^{(l-1)} + \mathbf{R}^{(l-1)} \cdot \bar{\mathbf{A}}_l, \\ \bar{\mathbf{A}}_l &= \text{Norm}_{\text{row}}(\text{Avg}_{\text{gh}}(\mathbf{A}_l^+) - \mathbb{I})/2 + \mathbb{I}/2, \end{aligned}$$

therein, it begin with the initialization $\mathbf{R}^{(0)} := \mathbb{I}$, Norm_{row} is the normalization ($\mathbf{p} = 1$) across horizontal rows of matrix, \mathbb{I} is the identical matrix and we count the $\mathbf{R}^{(L)}$ end up at layer \mathbf{L} as the final attribution. In our application context, these attributions prepare the granular token-to-token salience scores for both detailed and explainable semantic propagation measurement, meanwhile need time complexity to execute than others.

3.2 Uncertainty Recalibration

Providing with abovementioned prepared attribution matrix \mathbf{R} (also row-normalized) after LLM’s inference, as detailed demonstration in Figure 2, we convert salience to uncertainty score of each token and aggregate them as the following steps. Firstly, we sample \mathbf{N} times from the LLM, which empowers uncertainty to appear between the attribution matrices $\{\mathbf{R}_1, \mathbf{R}_2, \dots, \mathbf{R}_N\}$, $\mathbf{R}_n \in \mathbb{R}^{T_n}$ of different generations, \mathbf{T}_n is the total length of input tokens added up with output tokens and \mathbf{T}_0 in the length of input tokens. In these attribution matrices, the region of our interest (**R.O.I.**) is the columns from the first column to the \mathbf{T}_0 column in rows from the \mathbf{T}_0 row to the \mathbf{T}_n row, because they represent each input token’s semantic contribution in the propagation process of each output token. These regions reflect how the input token propagates its own semantics into high-level semantics, which are selected by generated tokens. That is:

$$\mathcal{R}_{roi} = \{\mathbf{R}_{n, [\mathbf{T}_0:\mathbf{T}, 1:\mathbf{T}_0]} | n \in \{1, 2, \dots, N\}\}. \quad (1)$$

Here, $[\cdot : \cdot, \cdot : \cdot]$ is the continuous submatrix selection operation. Thus, the uncertainty of semantic propagation can be derived by measuring the discrepancy of these regions in different sampling channels. Then, we average different columns across the rows of each attribution submatrix (col refers to columns dimension):

$$\bar{\mathcal{R}}_{roi} = \text{Avg}_{\text{col}}(\mathcal{R}_{roi}) \in \mathbb{R}^{N \times T_0}. \quad (2)$$

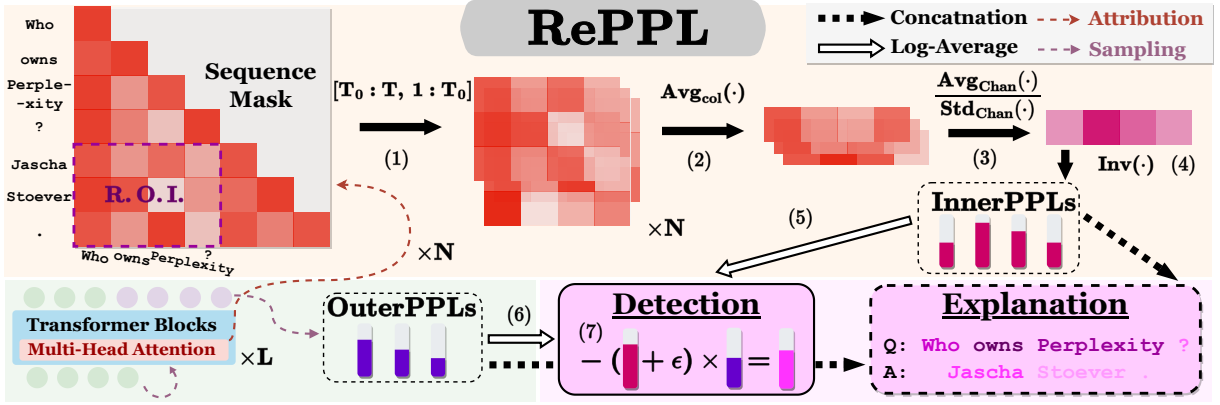


Figure 2: Detailed illustration of **RePPL** computing process. (1) ~ (7) correspond to the same equations in paper. ‘**InnerPPLs**’ and ‘**OuterPPLs**’ with plural form to indicate token-wise confidence scores.

These attribution submatrices are condensed into vectors with T_0 length and N sampling channels. They express the average semantic propagation on all generated tokens, which also gets rid of the different generation lengths. To derive uncertainty in sampling channels, we choose the coefficient of variation that is scale-/unit-independent for undistorted uncertainty measurement. That is the following equation (chan refers to channels dimension):

$$\mathbf{r} = \frac{\text{Std}_{\text{chan}}(\bar{\mathcal{R}}_{\text{roi}})}{\text{Avg}_{\text{chan}}(\bar{\mathcal{R}}_{\text{roi}})}, \quad (3)$$

it directly uses the standard deviation (Std) divided by the average. The coefficient of variation vector \mathbf{r} quantifies the uncertainty of different input tokens. Next, we use the inverse function to transform this coefficient of variation vector to pseudo-confidences similar to logit-based probabilities. This transformation is:

$$\hat{\mathbf{p}} \in [0, 1]^{T_0}, \hat{p}_i = \text{Inv}(r_i) = \frac{1}{1 + r_i^\alpha}. \quad (4)$$

In the above equation, α is the hyperparameter that controls uncertainty scaling. Subsequently, similar to the Perplexity (Ren et al., 2023), we adopt log rescaling and length-as-divisor average of $\hat{\mathbf{p}}$ to calculate the total score in inner side semantic propagation:

$$\text{InnerPPL} = -\frac{1}{T_0} \sum_{i=1}^{T_0} \log(\hat{p}_i). \quad (5)$$

Hence, we named as **InnerPPL**. The \log conversion will enlarge the significant part of the uncertainty and more validly take it into account for hallucination scores. For the outer part, given the

g -th generated token confidence \mathbf{p}_g and generation length S_g at the greedy decoding, we compute the overall generation uncertainty **OuterPPL** as:

$$\text{OuterPPL} = -\frac{1}{\bar{S}} \sum_{g=1}^{S_g} \log(\mathbf{p}_g), \quad (6)$$

\bar{S} is the average length of N sampled generations, and the only difference between our **OuterPPL** and original PPL is different divisors. The rationale behind this divisor is that we observe (as shown in Figure 3) that the generation length of the greedy decoding is basically shorter than sampling generations when LLM is certain. On the contrary, if LLM tends to hallucinate, the greedy path is roughly equal to most sampling paths. Thus, this divisor plays the role of a reward or penalty factor to make outer uncertainty more discriminative. Fi-

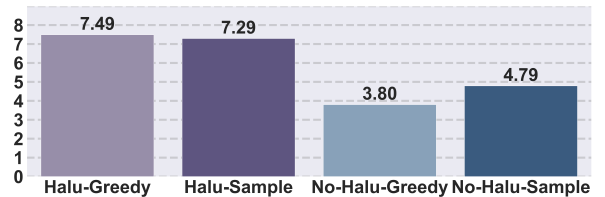


Figure 3: Length of greedy (‘Greedy’) outputs and average length of sampled generations (‘Sample’) of 1000 examples in TriviaQA. ‘Halu’ is hallucinated ones, and ‘No-Halu’ is the not hallucinated ones.

nally, **RePPL** is the multiplication form of these two scores, which means recalibration of uncertainty from the two aspects. It is:

$$\text{RePPL} = -(\text{InnerPPL} + \epsilon) \times \text{OuterPPL}, \quad (7)$$

ϵ is the presetted bias term, which is the default value to express correct uncertainty in case **InnerPPL** is 0 but **OuterPPL** is still large. In general,

we choose $\frac{1}{10} \sim \frac{1}{5}$ of average **InnerPPL** value for ϵ . Since the multiplication form of our hallucination score comprehensively considers uncertainty in semantic propagation and language generation, it is capable of hierarchical division when **InnerPPL** is large but **OuterPPL** is small, or vice versa. This trait equipped our method more layered distinctness for better detection. As for the uncertainty (or confidence) scores that granularly express token-wise contribution to hallucination, we collect them from the above computing process as an explanation of hallucination. These token-by-token scores attribute uncertainty rather than salience, thus figure out which input tokens trigger hallucination and which output tokens are more likely to be the hallucination.

4 Evaluation

4.1 Experimental Setup

Datasets. Question answering (QA) is the most common scenario for LLM-based applications. We choose four widely used QA datasets to evaluate our proposed hallucination score. Two of them are closed-book QA datasets, i.e., TriviaQA (Joshi et al., 2017) and Natural Questions (NQ) (Kwiatkowski et al., 2019). TriviaQA is a dataset that assembles trivia knowledge questions with precise answers, we select 9960 QA pairs in the validation split of *rc.noncontext* subset after deduplication. NQ is a dataset composed of Google search-based QA pairs. We choose the 3610 QA pairs in the validation split for evaluation, same as Chen et al. (2024). The other two are open-book QA datasets, i.e., CoQA (Reddy et al., 2019) and SQuAD (Rajpurkar et al., 2016). CoQA is a dataset about conversational QA, we utilize the development split of CoQA with 7983 QA pairs for our experiment. As for SQuAD, it is a reading comprehension dataset, and we take the development-v2.0 split with 5928 QA pairs (with filter condition *is_impossible=True*). All of the above subset selections are the same as prior work of Chen et al. (2024).

Target Models. We choose three representative open-source models Llama-3.1-8B-Instruct (Grattafiori et al., 2024), Qwen2.5-7B-Instruct, and Qwen2.5-14B-Instruct (Yang et al., 2024) for experiments. Currently, they are widely used in diversified applications, and they are popular in various leadboards. Since they are high-performance instruction-finetuned models,

we believe their error can represent hallucination issues well in general application scenarios.

Inference Settings. On account of the instruction finetuned models, we equip them with a normal chat template described in Appendix A. For sampling-based methods, including ours, in line with prior works (Farquhar et al., 2024; Chen et al., 2024), we set the number of sampled generations $N = 10$, temperature $\mathcal{T} = 1.0$, sampling hyperparameters Top-K = 50 and Top-P = 0.99 to guarantee the randomness needed by these methods. These inference settings are both fair for comparison and practical for application.

Correctness Measure. Consistent with previous work (Chen et al., 2024), we take the output in greedy decoding as LLM’s canonical response to judge whether it is hallucinated. We follow Du et al.’s (2024) and Chen et al.’s (2024) work to use embedding similarity as a correctness measure for ground truth labeling. The sentence embedding of the LLM’s response and the standard answer of the QA pairs are extracted by the model all-MiniLM-L6-v2 (Reimers and Gurevych, 2019). We treat embedding similarity between the LLM’s response and the standard answers lower than 0.9 as hallucination. Besides that, we also supplement the experiment using ROUGE-L (f-measure) (Lin, 2004) as the correctness measure in Appendix B.

Evaluation Metrics. To comprehensively evaluate the performance of hallucination detection scores, similar to Chen et al. (2024), we examine them by three metrics. The first is the widely acknowledged area under the receiver operator characteristic curve (AUC). The second is accuracy at the classification threshold of deriving the maximum **G-Mean** value. G-Mean is defined as $\mathbf{G-Mean} = \sqrt{\text{TPR} \times (1 - \text{FPR})}$, where TPR is true positive rate and FPR is false positive rate. This accuracy is well recognized when evaluating classification performance in imbalanced situations. Lastly, we select Spearman Correlation to fairly compare the correlation between hallucination scores and ground truth labels. For these metrics, higher scores indicate better performance.

Baselines. We select six baselines for comparison. The logits-based methods include popular **Perplexity** (Ren et al., 2023), commonly applied OOD detection score **Energy** (Liu et al., 2020), and **P(True)** (Lin et al., 2022). The sampling-based

Models	Datasets Methods	CoQA			TriviaQA			NQ			SQuAD			ALL		
		AUC	Acc	Corr												
LLaMA-3.1-8B-Instruct	Perplexity	66.6	61.7	30.0	78.2	71.1	51.0	77.5	67.5	38.9	67.4	64.9	31.1	73.9	67.5	43.8
	Energy	64.4	59.6	26.5	67.6	62.6	33.7	66.3	65.3	26.2	69.4	64.1	33.4	69.1	63.4	35.8
	P(True)	64.0	60.2	25.8	75.8	69.6	48.7	69.1	67.0	33.2	64.4	60.4	25.7	71.5	65.8	40.9
	LNPE	72.1	65.7	39.9	80.2	73.0	55.2	78.1	68.1	42.8	69.7	67.2	35.1	76.8	70.1	49.5
	Semantic Entropy	74.5	70.6	43.2	73.6	69.4	43.9	67.9	69.0	24.3	66.7	68.6	31.1	73.9	70.4	44.0
	EigenScore	77.2	70.6	49.3	80.5	74.3	55.3	74.9	71.6	42.4	76.8	70.9	47.4	78.2	71.8	51.8
	RePPL (Ours)	85.2	77.4	61.8	86.0	78.6	63.2	79.3	69.9	47.4	76.0	71.7	45.1	83.6	76.3	60.0
Qwen-2.5-7B-Instruct	Perplexity	74.9	71.7	43.3	83.6	75.9	60.5	76.8	73.3	39.0	75.5	69.8	43.5	80.6	74.3	55.3
	Energy	53.0	51.8	9.7	76.3	69.3	50.9	64.8	57.1	35.6	59.1	57.7	14.3	66.1	61.0	33.8
	P(True)	54.7	53.3	10.3	79.7	74.3	55.2	67.5	68.8	22.3	56.8	57.0	12.3	70.6	65.3	39.8
	LNPE	76.8	71.9	46.8	83.6	76.1	61.2	77.4	69.1	42.4	76.1	70.5	44.6	81.2	74.3	56.9
	Semantic Entropy	71.3	69.2	39.3	76.7	76.2	48.3	72.1	76.9	24.5	60.8	54.6	19.7	74.5	72.8	46.0
	EigenScore	83.0	76.2	58.4	82.5	75.2	60.2	79.5	69.7	49.2	77.3	73.4	46.9	82.5	75.2	59.8
	RePPL (Ours)	83.5	77.0	58.4	84.6	76.3	62.4	80.0	73.6	45.8	78.1	71.9	47.8	83.7	75.9	60.9
Qwen-2.5-14B-Instruct	Perplexity	74.5	73.6	39.2	81.4	75.3	56.4	76.7	70.7	44.2	75.7	71.5	45.2	78.0	73.4	49.4
	Energy	51.3	48.9	18.3	62.5	58.6	26.5	58.0	56.8	28.9	60.8	58.6	18.4	52.8	50.2	11.4
	P(True)	58.9	54.4	20.9	70.1	68.1	41.7	63.8	66.6	23.9	53.2	52.9	8.3	60.0	57.4	23.3
	LNPE	76.1	75.8	41.3	82.4	75.5	58.6	77.2	72.2	46.8	76.9	71.4	47.4	79.1	74.2	51.4
	Semantic Entropy	66.2	53.6	27.9	73.9	72.9	47.2	71.7	71.4	31.9	63.2	59.7	26.1	69.3	64.1	37.7
	EigenScore	82.5	72.2	49.7	81.8	75.5	59.1	77.7	70.8	51.7	80.4	73.0	53.5	81.6	73.2	56.7
	RePPL (Ours)	79.7	76.6	43.0	84.8	76.8	62.2	80.0	71.7	51.4	81.3	74.4	54.7	82.5	75.7	56.0

Table 1: Evaluation results of different methods on various datasets using AUC, accuracy at corresponding threshold derived max G-Mean value (Acc), and Spearman Correlation (Corr) metrics. We also present performance on the 4 datasets’ merge in the “ALL” columns. The highest values are highlighted in bold, and all values are in percentages.

methods contain Length-normalized Predictive Entropy (LNPE) (Malinin and Gales, 2021), broadly acknowledged Semantic Entropy (Farquhar et al., 2024) and EigenScore (Chen et al., 2024). The latter two are strong baselines. These baselines’ implementation is detailed in Appendix A.

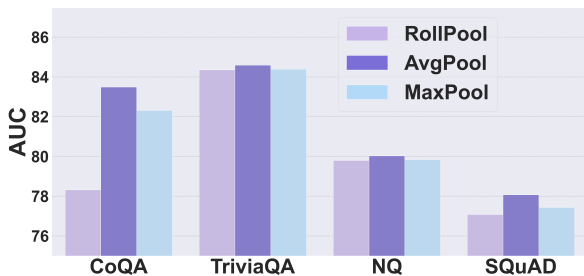


Figure 4: Comparison of base attribution strategies.

4.2 Main Results

We select **AvgPool**, $\alpha = 1.0$, and $\gamma = 0.005$ for our method. Table 1 reports the main results about the performance comparison of our **RePPL** and other baseline methods. From these results, we find that: (1) Our method achieves strong performance on hallucination detection. We reach the average AUC of **0.813** and **74.65%** accuracy at maximum G-Mean value on all individual datasets and all models. In addition, we also achieve an average

AUC of **0.833** across 4 datasets (on the merge of 4 datasets). (2) Our method outperforms baselines, especially the strong baseline Semantic Entropy and EigenScore. Out of **36** evaluated metrics of individual datasets, our method ranks first in **25**, demonstrating its overall superiority. Compared to EigenScore, which ranks second and performs an average AUC of 0.795 & 72.78% average accuracy, Our method takes the leading position of detection performance by 2% improvement. And we also outperform in the merge of all datasets. (3) Our method exhibits high generalization across different datasets. Our method basically guarantees the AUC higher than 0.75, and the accuracy higher than 70%. (4) Our method also demonstrates good adaptability among different models, and it can scale to larger models like **Qwen2.5-14B-Instruct**. Therefore, **RePPL** owns strong hallucination detection performance. And it firmly supports the foundation of its explainability.

4.3 Ablation Studies

Computation Variation. To further verify the effectiveness of our proposed method, we conduct ablation experiments on Qwen2.5-7B-Instruct and illustrate them in this section. Firstly, we compare **InnerPPL** & **OuterPPL** and the vanilla perplexity version of our method (multiplying original Per-

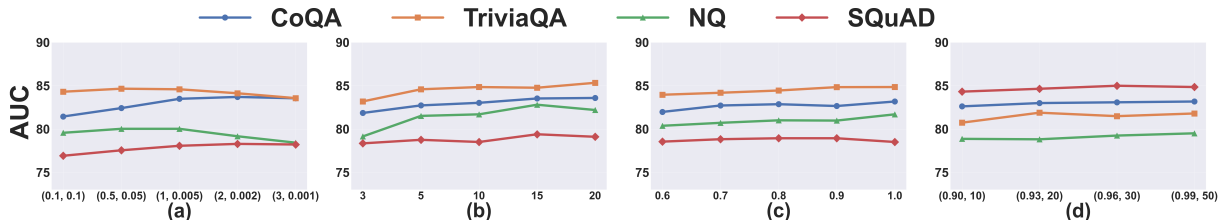


Figure 5: Performance under different hyperparameters. They are (a) our rescaling hyperparameter group (α, γ) , (b) number of Generation N , (c) temperature \mathcal{T} , (d) sampling hyperparameter group (Top-P, Top-K).

plexity in Equation (7)) to prove the efficacy of our design. As Table 2 demonstrated, **RePPL** certainly improves performance over all its computational variations. Besides, **InnerPPL** and **RePPL** (Perplexity) derived from the original perplexity perform well individually.

Ablations	Datasets			
	CoQA	TriviaQA	NQ	SQuAD
InnerPPL	83.5	80.1	76.3	75.3
OuterPPL	78.2	84.1	77.7	76.1
RePPL (Perplexity)	82.1	84.5	79.6	77.7
RePPL	83.8	84.6	80.0	78.1

Table 2: Ablation studies on Qwen2.5-7B-Instruct.

Attribution Strategies. We also investigate the influence of different attribution methods in Figure 4. An unexpected finding is that **AvgPool** performs best across all comparisons. Meanwhile, considering the lower computational complexity of **AvgPool**, we recommend it as the approach to derive the attribution map in our method.

Hyperparameters (α, ϵ) . As for the hyperparameter group (α, γ) , the ablation results are shown in Figure 5(a). It indicates that our method remains robust under different hyperparameter settings. Given that $(1.0, 0.005)$ achieves the best overall performance across 4 datasets, we recommend it as the default setting of our method.

4.4 Sensitivity to Sampling Hyperparameters

In this section, we extend our analysis to sensitivity to randomness in sampling, which is controlled by the following decoding hyperparameters. For efficiency considerations, a random one-fifth subset was taken from each dataset. The observed performance differs by no more than 1.5% from the main results. As Figure 5 (b) (c) (d) shows, randomness at different sampling hyperparameters affects our performance. However, this effect is limited as these curves display a moderately gradual ascent

from lower randomness hyperparameters to higher ones. It indicates that our method is robust.

5 Explainability Analysis

5.1 Faithfulness Test

In line with previous XAI works (Hao et al., 2021; Chefer et al., 2021; Achteibat et al., 2024), we assess explanation faithfulness via perturbation tests that progressively mask low-scoring tokens. The difference is that the assessment here focuses on which explanation more effectively highlights tokens that are more prone to inducing model hallucinations (uncertainty), rather than those that contribute more to the output (salience), hence, it needs detection performance as the indicator. A smaller detection performance drop across masking ratios indicates greater faithfulness, and the absolute performance itself also reflects explanation reliability. To assess

Exp. Scores	TriviaQA				SQuAD			
	0%	25%	50%	75%	0%	25%	50%	75%
Raw Logits	66.9	67.1	65.5	63.7	51.2	51.0	50.8	50.2
AvgPool	60.0	60.0	59.3	57.6	51.3	51.5	52.0	53.0
MaxPool	62.6	62.7	62.3	62.4	50.2	50.8	52.1	54.5
RollPool	55.4	55.3	55.2	55.0	48.0	48.2	48.9	50.5
InnerPPL	79.7	79.4	79.1	78.6	74.2	73.9	73.8	73.2

Table 3: Faithfulness test on TriviaQA and SQuAD, AUC metric. Percentages are different masking ratios.

the faithfulness of identifying uncertainty-inducing tokens, we conduct the test in the input space (corresponding to log rescaled uncertainty score that consists **InnerPPL**), using one-fifth random subsets from TriviaQA and SQuAD. As for comparison, we take the raw logits in throughput of the input tokens, salience-oriented attribution scores of three pooling strategies (using the form in Section 3.1) as explanation scores baselines. We steply mask these hallucination scores at ratios of 0%, 25%, 50%, and 75% and use the AUC metric for evaluation. Table 3 depicts a slight decrease in our method’s performance at different masking ratios,

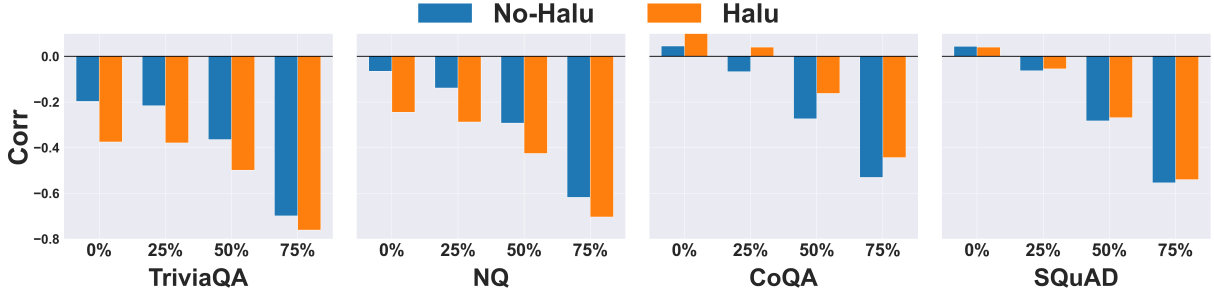


Figure 6: Average Spearman Correlation (Corr) between salience and uncertainty. Percentages are different masking ratios. As can be seen, the negative average correlation is large at 75% masking ratios. On the QA datasets with context, this negative correlation is smaller in hallucinated ones while larger on the datasets without context.

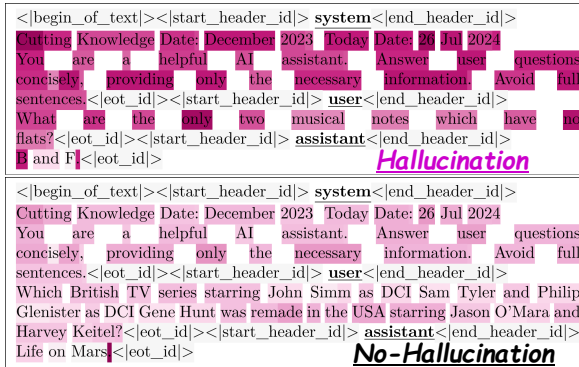


Figure 7: Visual explanations of the whole QA process on TriviaQA. The upper one is detected as a hallucination by RePPL. The lower one is non-hallucinated. Here, we mask the special token for better presentation.

which proves the primary capability of rightfully attributing significant uncertainty-inducing tokens. On the contrary, all baselines show erratic drops, which show their inability to explain. Our method even keeps the high performance at the 75% ratio. This suggests its capacity to truly concern uncertainty-inducing tokens related to hallucinations.

5.2 Visual Explanation for Hallucination

As mentioned in Section 3.2, we concatenate uncertainty scores that consist InnerPPL and OuterPPL as a token-wise and visualizable hallucination explanation. We take the log-rescaled uncertainty degree for visualization in Figure 7, which demonstrates good distinctness. More visual explanations are displayed in Appendix C.

5.3 Salience and Uncertainty

Coincidentally, during the computation process of our method, we first gain attribution-based salience and then derive the uncertainty about hallucination. We computed the average Spearman Correlation

between salience scores and uncertainty scores at the same data scale as Section 4.3 (detailed in Appendix A.4). Results in Figure 6 demonstrate two noteworthy findings: (1) **Uncertainty is negatively correlated to salience.** The negative correlation indicates uncertainty that induces hallucination, bringing chaos to the correct attention pattern. (2) **This correlation corresponds to different hallucination types.** The different average correlation on the dataset with/without context illustrates a discrepant hallucination pattern about factual (external) and contextual (internal) ones. Overall, these findings describe the disorder in the chaotic attention pattern when LLM tends to hallucinate. And demonstrate the potential usage of our explanation scores as a viable tool.

6 Conclusion

In conclusion, we are motivated by the explainability limitations of the current hallucination detection method, and introduce a fresh perspective to exploit uncertainty in semantic propagation and language generation. Based on that, we propose our RePPL to utilize the discrepancy between the attribution of different sampled generations and combine refined generation confidence. These designs equip our method with our hierarchical distinctness for better detection and token-level uncertainty correspondence for explanation. The experiments indicate that our method achieves strong detection performance, and it is able to highlight uncertainty-inducing tokens as an explanation. From the macro-level, it helps us to discover the chaotic patterns leading to hallucination. We hope our insights, even drawbacks, can better motivate future research in this domain to better tackle the hallucination of LLM and build more trustworthy AI systems.

Limitations

Our method is inherently limited by the following two drawbacks: (1) It mainly captures uncertainty-based hallucinations, whereas recent work (Yeh et al., 2025) highlights the existence of high-confidence hallucinations that slightly fall outside this range. (2) Its explanation is relatively coarse. This is partly due to the trade-off in time complexity, as the chosen attribution methods are different from general pooling of raw attention maps, which favors efficiency over the finer granularity offered by more computationally intensive state-of-the-art methods. (3) Our findings in Section 5.3 are also preliminary, which mainly embodies its potential utility. It requires more comprehensive statistical investigations at a larger scale. However, these drawbacks also point out valuable directions, such as unifying perturbation and sampling for more precise attribution. We believe our insights would gain better implementation by overcoming these limitations in future studies.

References

- Samira Abnar and Willem H. Zuidema. 2020. [Quantifying attention flow in transformers](#). In *Proceedings of the 58th Annual Meeting of the Association for Computational Linguistics, ACL 2020, Online, July 5-10, 2020*, pages 4190–4197. Association for Computational Linguistics.
- Reduan Achtibat, Sayed Mohammad Vakilzadeh Hatefi, Maximilian Dreyer, Aakriti Jain, Thomas Wiegand, Sebastian Lapuschkin, and Wojciech Samek. 2024. [Attnlrp: Attention-aware layer-wise relevance propagation for transformers](#). In *Forty-first International Conference on Machine Learning, ICML 2024, Vienna, Austria, July 21-27, 2024*. OpenReview.net.
- Hila Chefer, Shir Gur, and Lior Wolf. 2021. [Generic attention-model explainability for interpreting bimodal and encoder-decoder transformers](#). In *2021 IEEE/CVF International Conference on Computer Vision, ICCV 2021, Montreal, QC, Canada, October 10-17, 2021*, pages 387–396. IEEE.
- Chao Chen, Kai Liu, Ze Chen, Yi Gu, Yue Wu, Mingyuan Tao, Zhihang Fu, and Jieping Ye. 2024. [INSIDE: llms’ internal states retain the power of hallucination detection](#). In *The Twelfth International Conference on Learning Representations, ICLR 2024, Vienna, Austria, May 7-11, 2024*. OpenReview.net.
- Xuefeng Du, Chaowei Xiao, and Sharon Li. 2024. [Halo-scope: Harnessing unlabeled LLM generations for hallucination detection](#). In *Advances in Neural Information Processing Systems 38: Annual Conference on Neural Information Processing Systems 2024, NeurIPS 2024, Vancouver, BC, Canada, December 10 - 15, 2024*.
- Fahimeh Fakour, Ali Mosleh, and Ramin Ramezani. 2024. [A structured review of literature on uncertainty in machine learning & deep learning](#). *CoRR*, abs/2406.00332.
- Sebastian Farquhar, Jannik Kossen, Lorenz Kuhn, and Yarin Gal. 2024. [Detecting hallucinations in large language models using semantic entropy](#). *Nat.*, 630(8017):625–630.
- Javier Ferrando, Oscar Balcells Obeso, Senthoran Rajamanoharan, and Neel Nanda. 2025. [Do I know this entity? knowledge awareness and hallucinations in language models](#). In *The Thirteenth International Conference on Learning Representations, ICLR 2025, Singapore, April 24-28, 2025*. OpenReview.net.
- Aaron Grattafiori, Abhimanyu Dubey, Abhinav Jauhri, Abhinav Pandey, Abhishek Kadian, Ahmad Al-Dahle, Aiesha Letman, Akhil Mathur, Alan Schelten, Alex Vaughan, et al. 2024. The llama 3 herd of models. *arXiv preprint arXiv:2407.21783*.
- Yaru Hao, Li Dong, Furu Wei, and Ke Xu. 2021. [Self-attention attribution: Interpreting information interactions inside transformer](#). In *Thirty-Fifth AAAI Conference on Artificial Intelligence, AAAI 2021, Thirty-Third Conference on Innovative Applications of Artificial Intelligence, IAAI 2021, The Eleventh Symposium on Educational Advances in Artificial Intelligence, EAAI 2021, Virtual Event, February 2-9, 2021*, pages 12963–12971. AAAI Press.
- Ziwei Ji, Delong Chen, Etsuko Ishii, Samuel Cahyawijaya, Yejin Bang, Bryan Wilie, and Pascale Fung. 2024. [LLM internal states reveal hallucination risk faced with a query](#). *CoRR*, abs/2407.03282.
- Mandar Joshi, Eunsol Choi, Daniel Weld, and Luke Zettlemoyer. 2017. [TriviaQA: A large scale distantly supervised challenge dataset for reading comprehension](#). In *Proceedings of the 55th Annual Meeting of the Association for Computational Linguistics (Volume 1: Long Papers)*, pages 1601–1611, Vancouver, Canada. Association for Computational Linguistics.
- Tom Kwiatkowski, Jennimaria Palomaki, Olivia Redfield, Michael Collins, Ankur Parikh, Chris Alberti, Danielle Epstein, Illia Polosukhin, Jacob Devlin, Kenton Lee, Kristina Toutanova, Llion Jones, Matthew Kelcey, Ming-Wei Chang, Andrew M. Dai, Jakob Uszkoreit, Quoc Le, and Slav Petrov. 2019. [Natural questions: A benchmark for question answering research](#). *Transactions of the Association for Computational Linguistics*, 7:452–466.
- Chin-Yew Lin. 2004. [ROUGE: A package for automatic evaluation of summaries](#). In *Text Summarization Branches Out*, pages 74–81, Barcelona, Spain. Association for Computational Linguistics.
- Stephanie Lin, Jacob Hilton, and Owain Evans. 2022. [Teaching models to express their uncertainty in words](#). *Trans. Mach. Learn. Res.*, 2022.

- Weitang Liu, Xiaoyun Wang, John D. Owens, and Yixuan Li. 2020. [Energy-based out-of-distribution detection](#). In *Advances in Neural Information Processing Systems 33: Annual Conference on Neural Information Processing Systems 2020, NeurIPS 2020, December 6-12, 2020, virtual*.
- Xiaogeng Liu, Nan Xu, Muhao Chen, and Chaowei Xiao. 2024. [Autodan: Generating stealthy jailbreak prompts on aligned large language models](#). In *The Twelfth International Conference on Learning Representations, ICLR 2024, Vienna, Austria, May 7-11, 2024*. OpenReview.net.
- Scott M. Lundberg, Gabriel G. Erion, and Su-In Lee. 2018. [Consistent individualized feature attribution for tree ensembles](#). *CoRR*, abs/1802.03888.
- Scott M. Lundberg and Su-In Lee. 2017. [A unified approach to interpreting model predictions](#). In *Advances in Neural Information Processing Systems 30: Annual Conference on Neural Information Processing Systems 2017, December 4-9, 2017, Long Beach, CA, USA*, pages 4765–4774.
- Huan Ma, Jingdong Chen, Guangyu Wang, and Changqing Zhang. 2025. [Estimating LLM uncertainty with logits](#). *CoRR*, abs/2502.00290.
- Andrey Malinin and Mark J. F. Gales. 2021. [Uncertainty estimation in autoregressive structured prediction](#). In *9th International Conference on Learning Representations, ICLR 2021, Virtual Event, Austria, May 3-7, 2021*. OpenReview.net.
- OpenAI. 2023. [ChatGPT](#). Version GPT-4, Large language model.
- Hadas Orgad, Michael Toker, Zorik Gekhman, Roi Reichart, Idan Szepkter, Hadas Kotek, and Yonatan Belinkov. 2024. [Llms know more than they show: On the intrinsic representation of llm hallucinations](#). *arXiv preprint arXiv:2410.02707*.
- Pranav Rajpurkar, Jian Zhang, Konstantin Lopyrev, and Percy Liang. 2016. [SQuAD: 100,000+ questions for machine comprehension of text](#). In *Proceedings of the 2016 Conference on Empirical Methods in Natural Language Processing*, pages 2383–2392, Austin, Texas. Association for Computational Linguistics.
- Siva Reddy, Danqi Chen, and Christopher D. Manning. 2019. [Coqa: A conversational question answering challenge](#). *Trans. Assoc. Comput. Linguistics*, 7:249–266.
- Nils Reimers and Iryna Gurevych. 2019. [Sentence-bert: Sentence embeddings using siamese bert-networks](#). In *Proceedings of the 2019 Conference on Empirical Methods in Natural Language Processing*, pages 3982–3992.
- Jie Ren, Jiaming Luo, Yao Zhao, Kundan Krishna, Mohammad Saleh, Balaji Lakshminarayanan, and Peter J. Liu. 2023. [Out-of-distribution detection and selective generation for conditional language models](#). In *The Eleventh International Conference on Learning Representations, ICLR 2023, Kigali, Rwanda, May 1-5, 2023*. OpenReview.net.
- Marco Túlio Ribeiro, Sameer Singh, and Carlos Guestrin. 2016. ["why should I trust you?": Explaining the predictions of any classifier](#). In *Proceedings of the 22nd ACM SIGKDD International Conference on Knowledge Discovery and Data Mining, San Francisco, CA, USA, August 13-17, 2016*, pages 1135–1144. ACM.
- Shengyang Sun, Changyou Chen, and Lawrence Carin. 2017. [Learning Structured Weight Uncertainty in Bayesian Neural Networks](#). In *Proceedings of the 20th International Conference on Artificial Intelligence and Statistics*, volume 54 of *Proceedings of Machine Learning Research*, pages 1283–1292. PMLR.
- Yanling Wang, Haoyang Li, Hao Zou, Jing Zhang, Xinlei He, Qi Li, and Ke Xu. 2024. [Faclens: Transferable probe for foreseeing non-factuality in large language models](#). *Preprint*, arXiv:2406.05328.
- Xilie Xu, Keyi Kong, Ning Liu, Lizhen Cui, Di Wang, Jingfeng Zhang, and Mohan S. Kankanhalli. 2024. [An LLM can fool itself: A prompt-based adversarial attack](#). In *The Twelfth International Conference on Learning Representations, ICLR 2024, Vienna, Austria, May 7-11, 2024*. OpenReview.net.
- An Yang, Baosong Yang, Beichen Zhang, Binyuan Hui, Bo Zheng, Bowen Yu, Chengyuan Li, Dayiheng Liu, Fei Huang, Haoran Wei, et al. 2024. [Qwen2. 5 technical report](#). *arXiv preprint arXiv:2412.15115*.
- Min-Hsuan Yeh, Max Kamachee, Seongheon Park, and Yixuan Li. 2025. [Can your uncertainty scores detect hallucinated entity?](#) *CoRR*, abs/2502.11948.
- Lei Yu, Meng Cao, Jackie C. K. Cheung, and Yue Dong. 2024. [Mechanistic understanding and mitigation of language model non-factual hallucinations](#). In *Findings of the Association for Computational Linguistics: EMNLP 2024, Miami, Florida, USA, November 12-16, 2024*, pages 7943–7956. Association for Computational Linguistics.
- Hanning Zhang, Shizhe Diao, Yong Lin, Yi Fung, Qing Lian, Xingyao Wang, Yangyi Chen, Heng Ji, and Tong Zhang. 2024. [R-tuning: Instructing large language models to say ‘i don’t know’](#). In *Proceedings of the 2024 Conference of the North American Chapter of the Association for Computational Linguistics: Human Language Technologies (Volume 1: Long Papers)*, pages 7106–7132.
- Yuji Zhang, Sha Li, Cheng Qian, Jiateng Liu, Pengfei Yu, Chi Han, Yi R. Fung, Kathleen McKeown, Chengxiang Zhai, Manling Li, and Heng Ji. 2025. [The law of knowledge overshadowing: Towards understanding, predicting, and preventing llm hallucination](#). *Preprint*, arXiv:2502.16143.

A More Details of Experiments

A.1 Implementation Details

We conduct all of our experiments on an NVIDIA H100 GPU, with full precision FP32. All of the implementations are based on transformers Library of Huggingface¹. And all generations include related internal states and attention maps are derived from the `.generate(...)` of `GenerateMixin` Class (Which is the part of the Model Class). In addition, attention maps can be returned with setting with the `attn_implementation="eager"` when loading the model's weights. For model weights of Llama-3.1-8B-Instruct², Qwen2.5-7B-Instruct³, Qwen2.5-14B-Instruct⁴, and the sentence embedding model all-MiniLM-L6-v2⁵, we choose the open-source weights from their Huggingface repositories. For the ROUGE metric, we select the standard implementation of Google Research⁶.

A.2 Inference Settings

Since we select the instruction-finetuned model for experiments, to more closely simulate practical scenarios, we adopt the chat template for generation. In the system prompt, we constrain the model to only answer key information by the instructions. As a result, the model's responses are closer to the standard answer of QA pairs. The input format of QA pairs is shown as follows:

Input Format (Without Context)

System Prompt: You are a helpful AI assistant. Answer user questions concisely, providing only the necessary information. Avoid full sentences.

User Prompt: <Question>

The input format with context is:

¹<https://github.com/huggingface/transformers>

²<https://huggingface.co/meta-llama/Llama-3.1-8B-Instruct>

³<https://huggingface.co/Qwen/Qwen2.5-7B-Instruct>

⁴<https://huggingface.co/Qwen/Qwen2.5-14B-Instruct>

⁵<https://huggingface.co/sentence-transformers/all-MiniLM-L6-v2>

⁶<https://github.com/google-research/google-research/tree/master/rouge>

Input Format (With Context)

System Prompt: You are a helpful AI assistant. Answer user questions based on provided context concisely, providing only the necessary information. Avoid full sentences.

User Prompt: Context: <Context> Question: <Question>

A.3 Baseline Implementation

Perplexity. We compute perplexity as the following equation:

$$\text{PPL} = -\frac{1}{S} \sum_i^S \log(p),$$

here, S is the length of generation and p is logits of generation tokens.

Energy. Energy score is the result of exp-log rescaling:

$$\text{Energy} = \frac{1}{S} \sum_{i=1}^S \log\left(\sum_j \exp(p)\right),$$

which protrude the most uncertain logits.

P(True). It gives LLM a prompt to let LLM answer the question about whether the candidate answers hallucinate. We prompt LLM as follows:

Prompt of our Implementation of P(True)

System Prompt: You are a helpful assistant. You are asked to determine whether the possible answer correctly responds to the entire question, which may include context.

User Prompt: Entire Question (may include context): <Question>\n Possible answer: <Candidate Response>\n Does the possible answer correctly respond to the question above? Answer 'Yes' or 'No' only:

Then, if the "Yes" token (or equivalent tokens) appears in answers, we count the probability of this token $P(y = \text{"Yes"})$ as the hallucination score for detection.

Length-Normalized Predictive Entropy (LNPE). LNPE proposes to measure sequence-level uncertainty by calculating the expectation of uncertainty in multiple generations, which is mathematically

Models	Datasets Methods	CoQA			TriviaQA			NQ			SQuAD			ALL		
		AUC	Acc	Corr												
LLaMA-3.1-8B-Instruct	Perplexity	70.4	65.0	34.6	78.5	71.3	53.7	74.8	69.1	42.9	71.2	65.8	33.8	76.2	69.5	47.1
	Energy	68.1	62.1	30.9	68.0	63.6	35.6	65.3	62.7	28.8	70.7	66.2	35.4	71.9	66.0	39.7
	P(True)	66.4	61.6	29.6	77.9	71.1	50.7	69.3	65.8	35.6	68.6	61.0	27.5	74.4	68.1	44.0
	LNPE	75.4	68.1	43.6	81.0	73.4	56.9	76.1	69.5	43.1	73.5	70.7	37.7	79.3	72.4	52.1
	Semantic Entropy	75.3	70.0	44.2	75.2	69.2	44.3	66.1	64.1	25.7	71.6	73.2	33.3	76.1	70.7	45.5
	EigenScore	79.0	73.8	49.0	80.8	73.7	55.2	71.9	70.4	33.6	80.4	73.4	51.9	79.2	71.2	51.1
	RePPL (Ours)	83.5	77.0	60.6	85.2	76.9	62.5	75.3	69.4	37.9	76.0	70.8	48.1	82.8	75.5	58.9
Qwen-2.5-7B-Instruct	Perplexity	74.4	67.6	44.9	83.5	75.6	60.4	75.5	69.6	38.8	74.1	69.1	46.9	81.2	73.0	58.1
	Energy	60.2	57.3	16.1	77.6	70.8	49.4	64.6	57.5	27.6	60.8	58.7	15.9	71.0	65.8	39.8
	P(True)	57.7	57.2	16.4	80.8	75.0	57.3	65.1	63.9	26.5	59.2	60.3	14.2	74.1	69.8	46.4
	LNPE	76.3	69.9	48.0	83.7	76.0	60.6	76.4	66.6	40.1	75.1	70.2	48.1	82.1	74.3	59.5
	Semantic Entropy	74.2	73.8	40.9	77.7	76.0	49.4	71.8	73.1	30.3	65.9	79.3	22.2	77.7	76.4	49.0
	EigenScore	81.7	76.0	56.4	82.6	75.9	57.7	77.4	72.1	37.4	78.3	74.6	50.6	82.8	76.5	58.3
	RePPL (Ours)	81.2	73.7	57.1	84.1	76.0	61.1	77.7	67.0	37.8	77.1	70.5	51.6	83.3	75.4	60.8
Qwen-2.5-14B-Instruct	Perplexity	72.8	66.9	44.9	80.8	73.2	57.0	74.3	68.0	38.7	75.0	67.7	49.2	77.0	70.3	52.6
	Energy	61.1	57.0	27.4	63.5	61.0	28.4	60.0	56.7	22.8	60.0	58.8	20.8	57.4	54.1	22.8
	P(True)	60.8	57.9	27.0	72.4	71.0	44.8	62.0	65.2	28.3	54.0	55.9	9.4	63.1	62.6	33.8
	LNPE	74.2	68.0	47.4	81.9	74.6	58.7	75.2	68.9	39.7	76.4	69.8	51.4	78.1	71.2	54.6
	Semantic Entropy	67.8	62.5	36.1	76.7	76.3	47.0	69.9	72.2	30.3	66.4	72.3	29.0	71.8	70.9	41.8
	EigenScore	80.1	72.2	56.0	82.6	77.2	57.1	76.4	72.2	37.0	81.5	74.4	58.5	81.4	74.9	56.0
	RePPL (Ours)	76.3	71.2	50.6	84.1	76.2	61.1	77.5	69.2	39.1	80.6	72.6	58.9	80.7	73.4	56.9

Table 4: Evaluation results of different methods on various datasets using AUC, accuracy at corresponding threshold derived max G-Mean value (Acc), and Spearman Correlation (Corr) metrics. All values are in percentages.

equivalent to the average of the PPL across different generations. It is computed as:

$$\text{LNPE} = -\frac{1}{N} \sum_{m=1}^N \frac{1}{S_n} \sum_{t=1}^{S_n} \log(p).$$

Here, $1, 2, \dots, n$ is the index of each generation in N times and the S_n is the corresponding generation length.

Semantic Entropy. The core idea of this method is to cluster the uncertainty of similar outputs then accumulate overall uncertainty that avoids distortion in the direct average accumulation. It is:

$$H_m = -\sum_{i=1}^{C_m} p_i \log p_i,$$

$$\text{Semantic Entropy} = \frac{1}{M} \sum_{j=1}^m H_j.$$

Therein, we have M clusters $1, 2, \dots, m$, each has C_m numbers of outputs which contain H_m semantic entropy of the cluster.

EigenScore. This estimates the hallucination degree of generated outputs based on the semantic dispersion in the sentence embedding space. It computes the covariance matrix of N generated sentence embeddings and then uses the log and determinant of the regularized covariance matrix to

capture the diversity and confidence of the generation. It is defined as:

$$\text{EigenScore} = \frac{1}{N} \log \det(\Sigma + \alpha \cdot \mathbf{I}_N),$$

where $\Sigma = \mathbf{Z}^\top \mathbf{J}_d \mathbf{Z} \in \mathbb{R}^{N \times N}$ is the centered covariance matrix of N sentence embeddings $\mathbf{Z} = [z_1, \dots, z_n] \in \mathbb{R}^{d \times N}$, $\mathbf{J}_d = \mathbf{I}_d - \frac{1}{N} \mathbf{1}_N \mathbf{1}_N^\top$, and $\alpha \cdot \mathbf{I}_N$ is a small regularization term added to make the covariance matrix full rank. z_n is the middle layer hidden state of the last token.

A.4 Details of Average Correlation

For Spearman Correlation computing, the significant value $p > 0.05$ ones are treated as 0 correlation, and when both the uncertainty score and salience score are masked as 0 at the same time for the same token, this pair is removed for correct computation.

B ROUGE-based Main Results

The results of ROUGE-L (f-measure) as the correctness measure are listed in Table 4, with the threshold 0.5. Our method achieves the best comprehensive performance over individual datasets and the merge of 4 datasets with different models.

C More Visual Explanations

We display 8 visual explanations on TriviaQA in Figure 8 and 4 visual explanations on SQuAD in Figure 9 (we mask the specific tokens for better presentation). As these figures show, distinct-



Figure 8: Visual explanations of the whole QA process on TriviaQA. The upper 4 are hallucinated ones, while the lower 4 are non-hallucinated ones.

ness between the hallucinated answers and the non-hallucinated answers is obvious. It also indicates

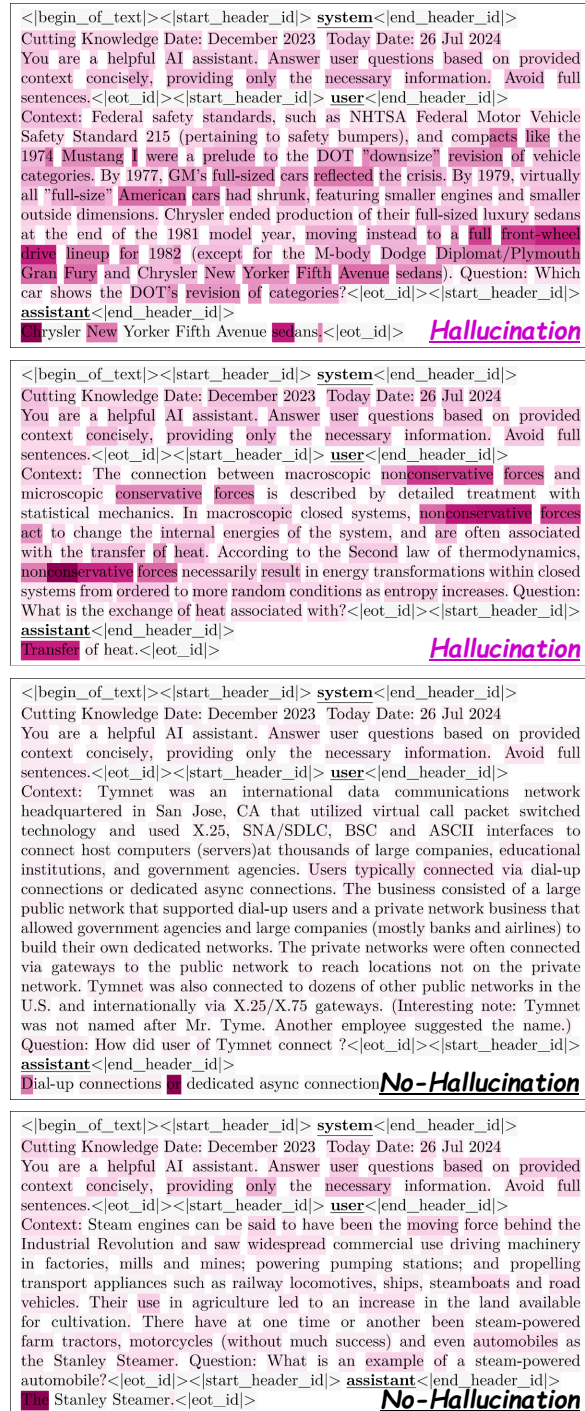


Figure 9: Visual explanations of the whole QA process on SQuAD. The Upper 2 are hallucinated ones, while the lower 2 are non-hallucinated ones.

that it is hard to detect hallucination with uncertainty in language generation alone.